Frequency-resolved photocurrent studies in amorphous germanium

R. KAPLAN[*], B. KAPLAN
Physics Division, Department of Mathematics and Science Education, Education Faculty, University of Mersin, Ciftlikkoy Campus, 33343 Mersin, Turkey

In-phase and in-quadrature frequency-resolved photocurrent (IP-FRPC and IQ-FRPC) measurements in amorphous (a-) Ge and a-GeSi thin films are reported as a function of excitation light intensity, wavelength, and applied dc electric field at room temperature. These measurements provide the carrier lifetime distributions directly. The in-quadrature signal is much more sensitive to phase inaccuracies than the in-phase signal. The lifetime of a-Ge and a-GeSi is found to be independent of excitation light intensity and applied electric field. We also present the exponent ν in the power-low relationship, $I_{ph} \propto G^{\nu}$, between light generation flux and photocurrent at different frequencies and wavelengths. It is found that the exponent, ν, has a sublinear intensity dependence with $0.55 < \nu < 0.90$. The exponent ν was also compared for IP-FRPC and IQ-FRPC outputs, and different materials, which supply information about recombination kinetics. The results are discussed on the basis of models proposed for the photocurrent studies.

1. Introduction

Amorphous silicon, germanium and their alloys have attracted considerable attention as promising new materials for photovoltaic and optoelectronic devices [1-5]. These applications, and many others, require optimisation of the electron and hole charge carrier recombinations and lifetimes [6-10]. They are dominated by the shallow and deep trapping centers which arise as a consequence of the disordered nature of the material.

The development of highly photosensitive narrow band-gap materials is one of the key issue in achieving high conversion efficiencies of amorphous silicon-based multijunction solar cells [11]. In that respect, amorphous silicon-germanium alloys are exremely useful materials as the band gap can be matched with the low energy region (< 1.7 eV) of the solar spectrum by varying the germanium content of the film. This material can be used effectively as the bottom layer of a tandem cell for improving stability and efficiency simultaneously. Hydrogenated amorphous silicon-germanium alloys (a-SiGe:H) are now being used to fabricate high efficiency tandem solar cells [12-15]. Althoug high efficiencies have been reported in this configuration, further improvement in the cell performance is limited due to poor efficiencies of the a-SiGe:H low band-gap cell.

Amorphous semiconductors usually exhibit a considerable density of localized energy levels within the forbidden gap, associated with defect states. These levels are generally the most efficient recombination centers, thus controlling the electrical transport properties.

In commercial applications of amorphous semiconductors such as solar energy conversion, electrophotography, and thin-film transistor arrays; carrier recombinations and lifetimes tend to be of critical importance. In many cases the mobility-lifetime product is used as a figure of merit for assessing material quality. Comparison between different specimens tend to be performed via light intensity dependence and lifetime measurements of room temperature photocurrent at the same illumination level.

The electronic properties of a-Ge and a-SiGe are somewhat poorer than the properties of a-Si. In particular, the defect densities and Urbach energies increase as the band gap decreases [16].

The use of modulated photocurrent is an attempt to describe the intensity and frequency variations of photocurrent by a consistent recombination model involving non-localized and localized states, provided that such variations appear to be reliable indicators of material properties. It is the fact that a consistent pattern of photocurrent behaviour is characteristic of a suprisingly large number of different types of amorphous semiconductors that makes this approach attractive.

The optical properties of materials are also important to determine their usage in optoelectronic applications. The optical band gap is usually dependent on the defects due to additional elements. The decreasing in direct band gap with increase in thickness is attributed to the formation of some defects leading to an increase in localised states in the band gap. Although the optical properties of a-Si:H and a-SiGe:H have been studied, the pure a-Ge, a-SiGe (not hydrogenated) and their comparison have not been studied in detail. Therfore the Ge based electronic materials are of particular interest.

Recombination is a key factor when describing photocarrier transport in amorphous materials because it strongly affects their electrical and optical responses at all levels of external excitation. In order to determine the quality of a semiconductor, an important parameter is the photocarrier lifetime, because it provides information on the distribution of defects exist in the material. The defects and impurity levels affect the carrier lifetime directly by supplying an alternative recombination path or by acting as trapping centers. The carrier lifetime distribution of a material, therefore, provides a sensitive measure of sample quality [17].

In the present work, we use frequency-resolved photocurrent (FRPC) spectroscopy to determine the carrier lifetimes of thermally evaporated a-Ge and a-SiGe thin films, at different light intensities and applied electric fields. The exponent ν in the power-low relationship, $I_{ph} \propto G^{\nu}$, between photocurrent and the carrier generation rate is determined at different frequencies and wavelengths. All the measurements were performed at room temperature. The results are discussed in terms of the proposed models that try to explain the photocurrent response in relation to the localizes states.

2. Experimental details

We produced the thin film of samples of a-Ge and a-SiGe by using a thermal evaporation unit. The materials used for these samples were from BDH chemicals with a high purity of 99.9992 %. Mostly we put co-planar Al or Au electrodes on the samples by using a suitable Al foil mask and the thermal evaporation unit. However, instead of using a crucible, the Al or Au ingots were evaporated directly from tungsten spiral. For electrode spacing, the different size Cu wires ranging between 0.1 mm and 0.2 mm were used as masks. Copper external leads were contacted with Ag paint. The current-voltage (I-V) measurements taken in dark proved that the contacts were perfectly ohmic. As noted previously [18], gold contacts perform better in injecting hole carriers and thus give larger photocurrents than aluminium contacts for these materials.

The samples were excited by a HeNe or an Ar laser. An acousto optic modulator (IntraAction Corp., Model AOM-125) was used to modulate the light sinusoidally in the frequency range of 10 Hz to 100 kHz. The modulation amplitude amounted to 46 % of the bias light intensity. The modulated photocurrent signal excited in this way was measured and analysed by a lock-in amplifier (SR 530 Stanford Research System). The intensity of the excitation light was reduced by a set of neutral density filters.

3. Theory

There are many transient photocurrent techniques [19-22] aimed primarily at probing the thermalization of photoexcited carriers in amorphous materials. On a longer time-scale, the decay of the photocurrent in the presence of recombination gives information about both deep recombination centers and traps in thermal equilibrium with the band. The response time is generally measured by measuring the time for the photocurrent to decay to some fraction of its initial value. Measurement of the modulation frequency dependence of the photocurrent is a complementary method of measuring the response time. Oscillatory modulation allows the investigation of details in the steady-state system response, whereas transient decay measurements average over a range of system conditions.

The frequency-resolved photocurrent (FRPC) spectroscopy technique has already been described [23-25]. In its simplest form, the optical excitation of a sample is modulated with a small amplitude sinusoid and the sample response to this modulation is measured either in-phase or in-quadrature to the phase of the excitation modulation, using a lock-in dedection. Logarithmically sweeping the modulation frequency then generates a lifetime distribution directly.

In the mathematical analyses of frequency-resolved spectroscoy (FRS) method, the in- phase FRS gives the integral of lifetime distribution, between the limits $\tau \sim (2\pi\omega)^{-1}$ and ∞, while the in-quadrature FRS gives the lifetime distribution directly. For a system with a single characteristic lifetime, τ, the in-quadrature FRS spectrum is a symmetric band, of half width 0.7 decades peaked at the frequency

$$f_{peak} = \frac{1}{2\pi\tau}. \tag{1}$$

The lock-in output from all lifetime components as the frequency is swept is given by

$$S(\omega) = \int_0^{\infty} P(\tau)s(\omega,\tau)d\tau \tag{2}$$

where $P(\tau)$ is the lifetime distribution, and $s(\omega,\tau)$ is the response function. For quadrature the lock-in response function is given by

$$s(\omega,\tau) = \frac{g_r}{(\omega\tau + \frac{1}{\omega\tau})} \tag{3}$$

while in-phase FRS, it takes the following form

$$s(\omega,\tau) = \frac{gr}{(1+\omega^2\tau^2)} \tag{4}$$

where g_r is the excitation rate. For comparison, the in-quadrature and phase response functions are represented together in Fig. 1. Althoug the in-quadrature FRS is the most useful form, the in-phase version can also give important additional information on the existence of fast processes beyond the time domain of the in-quadrature measurements. It is worth remembering that if one knows the quadrature response from $\omega = 0 \to \infty$ (which one does not), a Kramers-Kronig transform will give the in-phase

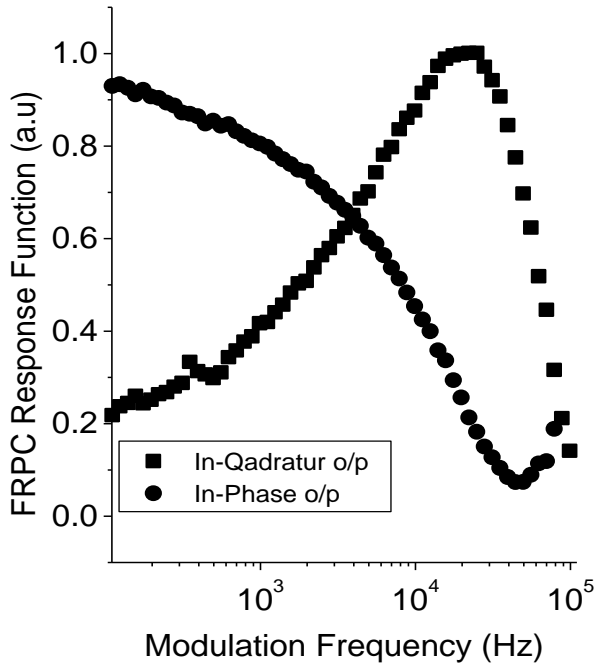response. That is all the information is in either response, if complete in ω.

Fig. 1. Freqency-resolved photocurrent (FRPC) response function for the in-quadrature (Eq. (3)) and in-phase (Eq. (4)) of a-Ge with a single well defined lifetime. Excitation: HeNe laser (632.8 nm, 2314 µW). Applied voltage: 500 V. (a.u, arbitrary units)

4. Results and discussion

The in-phase and in-quadrature frequency-resolved photocurrent (IP-FRPC and IQ-FRPC)) responses of the samples in the frequency interval between 10 Hz and 100 kHz were measured as a function of the intensity of the excitation light and applied voltages. Since the energy of the excitation light is much higher than the optical band gap of these materials, we assume that the carriers are photoexcited between extended states and then a trap limited recombination occurs at room temperature.

Fig. 2 shows IQ-FRPC and IP-FRPC spectra of a-Ge for different excitation intensities of HeNe laser (632.8 nm). Applied voltage was 500 V. Light intensities at the sample were varied from 248 µW to 2314 µW using neutral density filters. As seen from the IQ-FRPC spectra, there is only one single broad spectra which is almost independent of the excitation intensity. This means that there is only one characteristic lifetime.
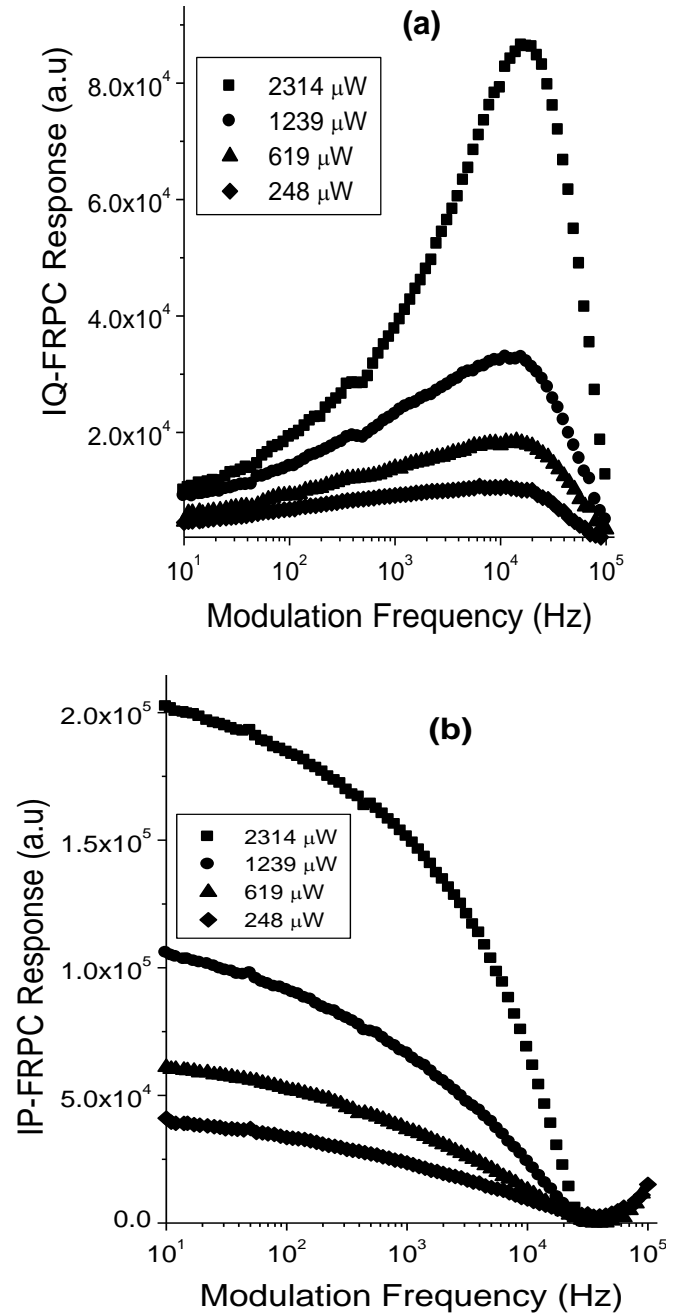

Fig. 2. (a) IQ-FRPC and (b) IP-FRPC spectra of a-Ge for different excitation intensities of HeNe laser (632.8 nm). Applied voltage is 500 V

Using Eq. (1), the lifetime, τ, is calculated as 10 µs. This is consistent with a sublinear intensity dependence of the photocurrent.

Fig. 3 shows the effect of applied voltage on the IQ-FRPC and IP-FRPC spectra in a-Ge. The applied voltage was varied from 100 V to 500 V. The excitation intensity was 2314 µW, from HeNe laser (632.8 nm). However the lifetime is also found to be independent of applied voltage and thus electric field.
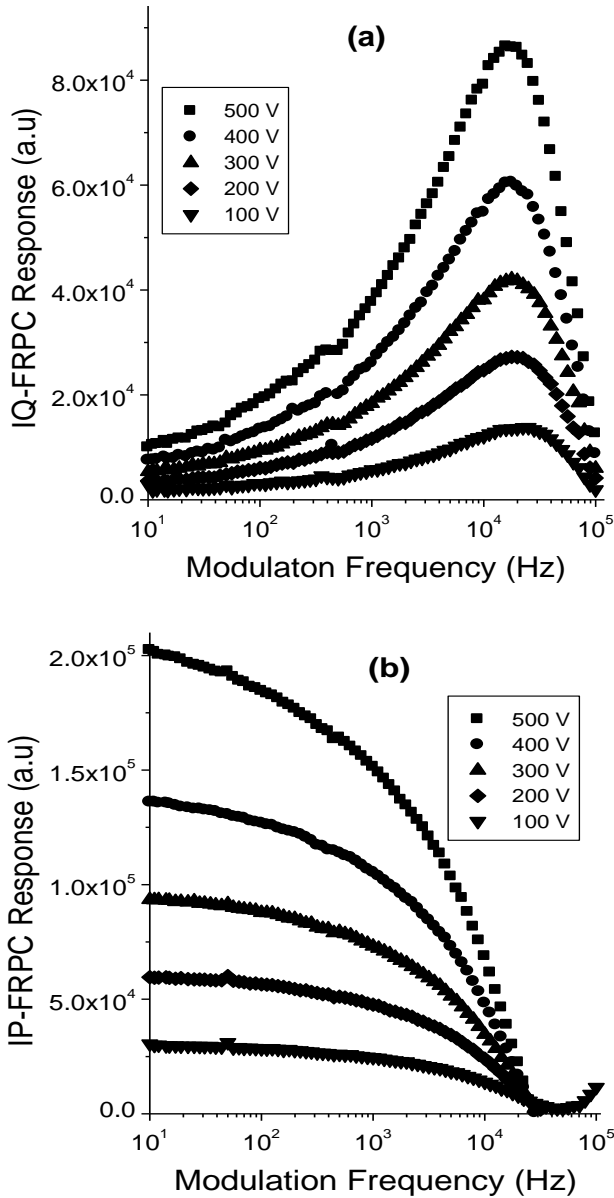
Fig. 3. (a) IQ-FRPC and (b) IP-FRPC spectra in a-Ge at different applied voltages. Excitation: HeNe (632.8 nm, 2314 µW)

Fig. 4. A comparison of IQ-FRPC (a) and IP-FRPC (b) spectra in a-Ge and a-GeSi. Excitation: HeNe (632.8 nm, 2314 µW)

The magnitude of IQ- and IP-FRPC decreases with decreasing voltages as expected. At room temperature, the photocarriers may be thermally ionized from recombination or trapping states, in which only one recombination path is present.

In Fig. 4, we compared the IQ- and IP-FRPC responses of a-Ge and a-SiGe under identical experimental conditions. The data were normaized to 1.0 for both output cases. The excitation intensity on the samples was 2314 µW. The applied voltage was 500 V.

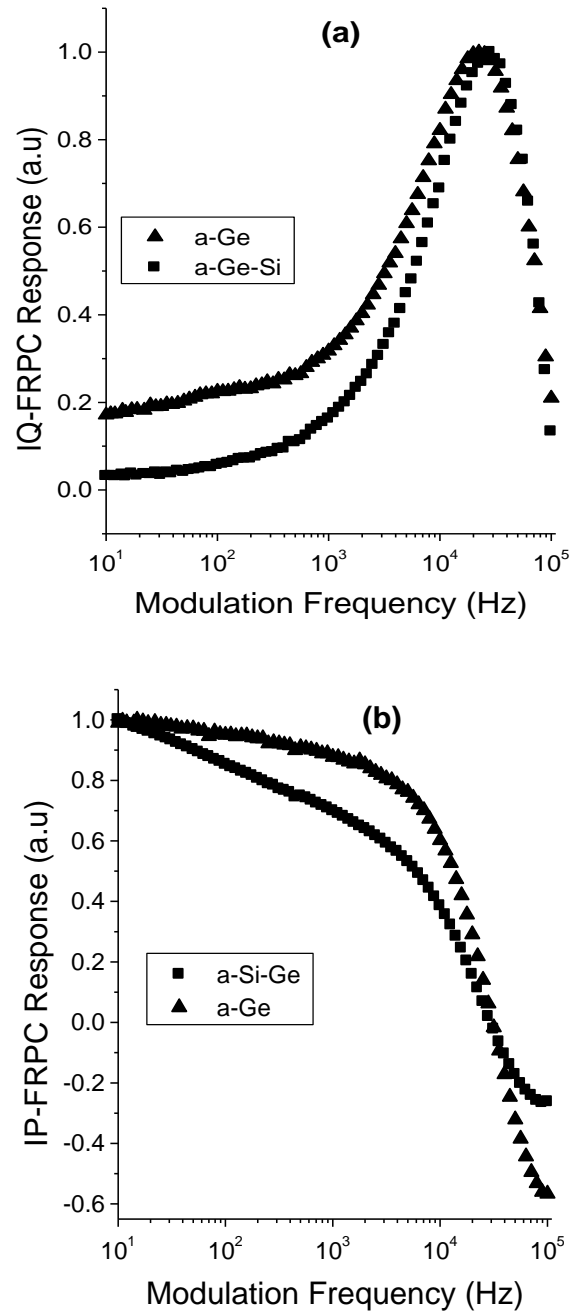As will be seen from Fig. 4, the spectra were peaked at 15.848 kHz and 22.748 kHz for a-Ge and a-GeSi, which corresponding to lifetimes of about 10 µs and 7 µs respectively. The sample of a-GeSi has a broader lifetime spectra than that of a-Ge due to the additional defect levels of Si. Photosensivity depends upon the lifetime of the excess carriers, which depends on the density of localized states in a particular material. Higher the density of localized states, lower will be the lifetime and photosensivity will, therfore, decrease. The reduction is the carrier lifetime when Si impurities are introduced is

due to an increase in the concentration of deep local centers, which retain carriers for a long time.

The next series of our experiments concerns the light intensity dependence of photocurrent, I_{ph}. For these measurements, the light intensity was increased in steps from 23.1 μW up to 2314 μW. Fig. 5 shows the light intensity dependence of photocurrent at two different outputs (IP and IQ) and modulation frequencies (10 Hz and 1 kHz). According to the power-law relatioship, $I_{ph} \propto G^\nu$, between light generation flux and photocurrent, the plot between $ln(I_{ph})$ and $ln(G)$ should be straight line. The exponent ν is calculated from the slope of the curve plotted in Fig. 5. The values of ν are found to be between 0.55 and 0.90 for both IP and IQ outputs. However, there are some frequency effect on the ν values.

It is now well known that the value of the exponent ν differs in various materials [27-29]. In most cases, a sublinear dependence is found and the exponent ν in the power-law relation $\left(I_{ph} \propto G^\nu\right)$ has quite complicated variations with photon energy, light intensity, temperature, modulation frequency and applied electric field [30-31].

Fig. 6 shows the photocurrent as a function of applied elctric field for IP and IQ outputs at two modulation frequencies of 10 Hz and 1 kHz. It will be seen that the points lie on a straight line of slope change, showing that the photoresponse of a-Ge is linear at room temperature. The IP o/p has the larger photocurrent than that of IQ o/p in magnitude. The slope of lines are different for different frequencies, which means that the different trap or recombination centers are exist in the energy gap.
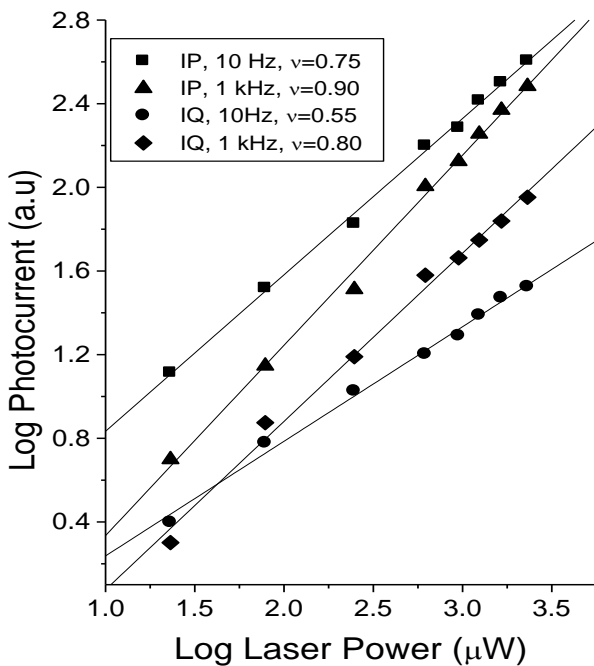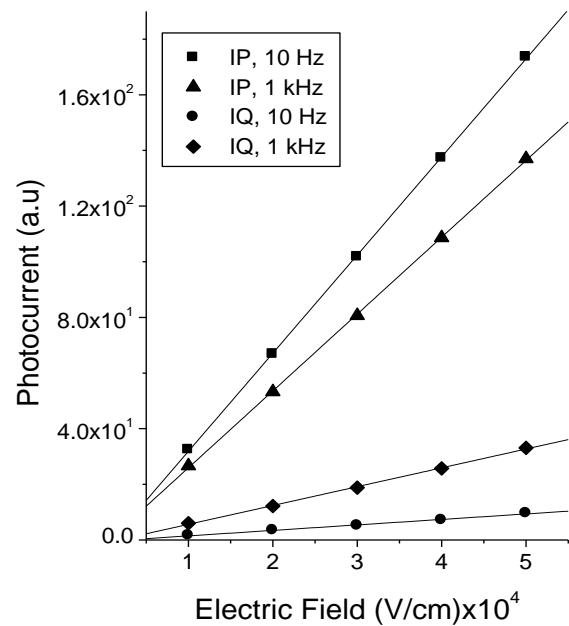

Fig. 5. Excitation (HeNe) intensity dependence of photocurrent of a-Ge at different IP and IQ outputs, and frequencies. The calculated values of exponent ν in $I_{ph} \propto G^\nu$ are also shown on the figure

Fig. 6. Electric field dependence of photocurrent of a-Ge at different IP and IQ outputs, and frequencies

Rose [26] suggests that $\nu = 1$ corresponds to monomolecular recombination and $\nu = 0.5$ to bimolecular recombination. However, in the case of continuous distribution of traps the value of ν may be anywhere between 0.5 and 1.0 depending on the light intensity and temperature range. In Fig. 5, the values of exponent ν lie between 0.55 and 0.90, indicating the presence of a continuous distribution of localized states in the energy gap. The exponet ν in power-law could qualitatively be associated with the amount of recombination centers located in the energy gap; a higher value of ν, in general, implies a higher rate of carrier recombination.

In Table 1, we compared the exponent ν (in $I_{ph} \propto G^\nu$), and carrier lifetimes of a-Ge and a-GeSi samples under identical conditions. Unfortunately the ν shows a complicated behaviour with wavelength for two different samples. As known, recombination is influenced both by material properties and by external parameters, such as light intensity, wavelength and modulation frequency which alter recombination kinetics. However, a complete set of equations describing the response of a photoconductor to light is practically intractable, an thus a full interpretation of these results unfortunately needs a sufficiently detailed knowledge of the recombination mechanism which is not presently available.

Table 1. Comparison of the exponent ν (in $I_{ph} \propto G^\nu$), and carrier lifetimes of a-Ge and a-GeSi samples under identical conditions. Exc.: HeNe (2314 μW), V_{app} = 500 V, T = 290 K

Sample	Exponent, ν			f_{peak}(Hz)	τ (μs)
Wavelength (nm)	476.5	528.0	632.8	632.8	632.8
a-Ge	0.59 ± 0.04	0.74 ± 0.03	0.70 ± 0.07	15848	10 μs
a-GeSi	0.73 ± 0.08	0.76 ± 0.02	0.75 ± 0.05	22748	7 μs

As will be seen from Table 1, the lifetime of a-GeSi is smaller than that of a-Ge. This result is in agreement with literature [11, referenced therein]. In a photoconductor the dificulties with the various lifetimes arise from the fact that photogenerated free carriers do not remain free until they recombine. Instead they become trapped and must be released from the traps thermally before they can recombine. Since in most photoconductors there are many more trapped carriers than free ones, the trapped carriers must not be forgotten in any consideration of lifetimes. Therefore, overall, shallow tail states tend to control the lifetimes of charge carriers, while deeper-lying centres near mid-gap (predominantly dangling bonds) act as recombination centres which limit the carrier lifetimes.

5. Conclusions

We have proposed an experimental method based on modulated photocurrent measurements to estimate the carrier lifetime, the exponent ν in $I_{ph} \propto G^\nu$ for evaporated a-Ge and a-GeSi samples with co-planar electrodes.

The recombination lifetime is one of the critical parameters in the search for cost-competitive photovoltaic technologies. Each technology has specific materials issues with respect to the role of recombination lifetime in potential success of that technology. In a-Ge and a-GeSi, the single lifetimes of 10 μs and 7 μs were determined respectively for the excitation light intensity of 2314 μW. These lifetimes were found to be material-dependent, but were found to be independent of the light intensity, the applied electric field and the excitation wavelength.

The information of recombination can be obtained in part by evaluating the modulated photocurrent versus light intensity characteristic. Therefore the exponent ν in the power-law, $I_{ph} \propto G^\nu$, was measured. The photocurrent is found to be sublinear in photon flux, with the exponent of 0.55-0.90 in the measured frequency, intensity and wavelength ranges. The ν was also compared for two samples of a-Ge and a-GeSi under the same experimental conditions. It was found to be a little excitation wavelength-dependence. Furthermore, IP and IQ outputs of the lock-in amplifier give a little different, but complicated results for ν. The excitation wavelength dependence of ν for both materials used can be related to the their light absorption profiles. The larger values of ν of a-Ge and a-GeSi show the presence of a continuous distribution of localized states in their energy band gap.

The shape of lifetime spectra reflects the trapping and the recombination of the photoexcited carriers. Lifetime measurements, in combination with the modulated photocurrent, I_{ph}, versus light intensity characteristic, allow a determination of the recombination mechanism. Our presented results show that the recombination occurs through the trap states at room temperature. Therefore the relese rate from traps controls both the lifetime and photocurrent.

References

[1] J. J. Sturm, E. J. Prinz, C. W. Magee, IEEE Electron. Device Lett. **12**, 303 (1991).

[2] T. L. Lin, T. George, E. W. Jones, A. Ksenzov, M. L. Huberman, Appl. Phys. Lett. **60**, 380 (1992).

[3] I. R. Hooper, E. Khorani, X. Romain, L. E. Barr, T. Niewelt, S. Saxene, A. Wratten, N. E. Grant, J. D. Murphy, E. Hendry, J. Appl. Phys. **132**, 233102 (2022).

[4] S. H. Lee, K. H. Min, S. Choi, H. E. Song, M. G. Kang, T. Kim, S. Park, Sol. Energy Mater. Sol. Cells **251**, 112144 (2023).

[5] M. M. A. Gamel, P. J. Ker, W. E. S. W. A. Rashid, H. J. Lee, M. A. Hannan, M. D. Z. B. Jamaludin, IEEE Access **9**, 37091 (2021).

[6] L. Bychto, M. Malinski, Optoelectronic Review **24**(2), 58 (2016).

[7] N. Schuler, T. Hahn, S. Schmerler, S. Hahn, K. Domich, J. R. Niklas, J. Appl. Phys. **107**, 064901 (2010).

[8] A. Castro-Chong, A. J. Riquelme, T. Aernouts, L. J. Benett, G. Richardson, G. Oskam, J. A. Anta, ChemPlusChem **86**, 1347 (2021).

[9] E. Gaubas, M. Bauza, A. Uleckas, J. Vanhellemont, Materials Science in Semiconductor Processing **9**, 781 (2006).

[10] D. Krisztian, F. Korses, G. Havasi, Sol. Energy Mater. Sol. Cells **260**, 112461 (2023).

[11] M. Güneş, M. E. D. Yavas, J. Klomfass, F. Finger, J. Mater Sci.: Mater Electron **21**, 153 (2010).

[12] S. Okamato, E. Maruyama, A. Terakawa, W. Shinohara, S. Nakano, Y. Hishikawa, K. Wakisaka, S. Kiyama, Sol. Energy Mater. Sol. Cells **61**, 85 (2001).

[13] Q. H. Fan, X. Liao, X. Xiang, C. Chen, G. Hou, X. Cao, X. Deng, J. Appl. Phys. D: Appl. Phys. **43**, 145101 (2010).

[14] J. W. Schuttauj, B. Niesen, L. Lofgren, M. B. Eymard, M. Stuckelberger, S. Hanni, M. Boccard, G. Bugnon, M. Despeisse, F. J. Haug, F. Meillaud, C. Ballif, Sol. Energy Mater. Sol. Cells **133**, 163 (2015).

[15] A. Dey, D. Das, Journal of Physics and Chemistry of Solids **154**, 110055 (2021).

[16] F. Zhong, J. D. Chen, J. Yang, S. Guha, Proc. Mater. Res. Soc. **336**, 493 (1994).

[17] E. Gubas, J. Vanhellement, Appl. Phys. Lett. **89**, 142106 (2006).

[18] J. M. Marshall, A. E. Owen, Philosophical Magazin **24**, 1281 (1971).

[19] S. P. Depinna, D. J. Dunstan, Philosophical Magazin B **50**, 579 (1984).

[20] T. M. Searle, Phil. Mag. Lett. **61**, 251 (1990).

[21] C. Main, D. P. Webb, R. Bruggemann, S. Reynolds, J. Non-Cryst. Solids **137-138**, 951 (1991).

[22] R. K. Ahrenkiel, N. Call, S. W. Johnston, W. K. Metzger, Sol. Energy Mater. Sol. Cells **94**, 2197 (2010).

[23] D. Wagner, P. Irsigler, D. J. Dunstan, J. Physics C: Solid State Physics **17**, 6793 (1984).

[24] M. A. Lourenco, K. P. Homewood, R. D. McLellan, J. Appl. Phys. **73**(6), 2958 (1993).

[25] M. A. Lourenco, K. P. Homewood, Semicond. Sci. Technol. **8**, 1277 (1993).

[26] A. Rose, Concept in Photoconductivity and Allied Problems, Krieger, 1978.

[27] R. Kaplan, Sol. Energy Mater. Sol. Cells **85**, 545 (2005).

[28] P. Hartnagel, T. Kirchartz, Adv. Theory Simul. **3**, 2000116 (2020).

[29] S. Zeiske, W. Li, P. Meredith, A. Armin, O. J. Sandberg, Cell Reports Physical Science **3**, 101096 (2022).

[30] R. Kaplan, B. Kaplan, Acta Physica Polonica **135**, 332 (2019).

[31] R. Kaplan, B. Kaplan, Optoelectron. Adv. Mat. **14**, 521 (2020).

*Corresponding author: rkaplan@mersin.edu.tr